Tapping the Gravitational Well: An Energetic Supernova Explosion with Boltzmann Neutrino Transport in General Relativity

Matthias Liebendörfer[1,2,3], Anthony Mezzacappa[2], Friedrich-Karl Thielemann[1,2],
O. E. Bronson Messer[2,3,4], W. Raphael Hix[2,3,4], Stephen W. Bruenn[5]

[1] *Department of Physics and Astronomy, University of Basel, Klingelbergstrasse 82, CH-4056 Basel Switzerland*

[2] *Physics Division, Oak Ridge National Laboratory, Oak Ridge, TN 37831-6354*

[3] *Department of Physics and Astronomy, University of Tennessee, Knoxville, TN 37996-1200*

[4] *Joint Institute for Heavy Ion Research, Oak Ridge National Laboratory, Oak Ridge, TN 37831-6374*

[5] *Department of Physics, Florida Atlantic University, Boca Raton, FL 33431-0991*

We report on the vigorous supernova explosion of a 13 $M_\odot$ star, obtained in a general relativistic spherically symmetric simulation based on Boltzmann neutrino transport. Contrary to the prevailing opinion, the shock revival is more efficient than in the corresponding Newtonian simulation, producing an explosion energy of 10^{51} erg (1 foe) at 187 ms after bounce.

I. BACK TO THE FUTURE?

In the pioneering days of supernova simulations (Colgate and White [1], May and White [2]) the consideration of general relativity (GR) was standard. The observable event of a stellar core collapse followed by a supernova explosion was an ideal application for the newly derived Einstein equations in spherical symmetry (Misner and Sharp [3]). Lindquist [4] formulated the GR Boltzmann equation, and Wilson [5] carried out simulations based on GR Boltzmann neutrino transport with parametrized neutrino interactions. This early epoch laid the foundation for our understanding of the supernova mechanism: A collapsing stellar iron core bounces at nuclear densities and launches a shock wave outwards through the infalling outer layers. The shock is energized by neutrinos diffusing out of the hot proto-neutron star and depositing a fraction of their energy in the shock dissociated matter via absorption on the free nucleons.

The early models have been refined in many respects. The equation of state evolved from simple polytropes to significantly more realistic models (Baron et al. [6], Lattimer and Swesty [7]). The neutrino opacities were improved (Schinder and Shapiro [8], Bruenn [9], Burrows and Lattimer [10]), and sophisticated multigroup flux-limited diffusion neutrino transport schemes were developed (Arnett [11], Bowers and Wilson [12], Bruenn [9], Myra et al. [13]).

However, improved approximations in the implementation of neutrino physics seemed to decrease the likelihood of successful explosions in spherical symmetry. The focus therefore switched on the one hand to the development of exact three-flavor Boltzmann neutrino transport (Mezzacappa and Bruenn [14,15]) and on the other hand to multidimensional phenomena. The controversial [16] inclusion of neutron finger convection into one-dimensional models produced explosions (Wilson and Mayle [17]) and established the delayed explosion scenario. Two-dimensional investigations of convection behind the shock and in the proto-neutron star followed with mixed results (Herant et al. [18], Miller et al. [19], Herant et al. [20], Burrows et al. [21], Janka and Müller [22], Keil et al. [23], Mezzacappa et al. [24]).

In the search for a robust supernova mechanism, attention was directed toward simulations in the nonrelativistic (NR) limit, because explosions in GR seemed to be less likely in the selective picture that the deeper shock formation would produce larger dissociation losses and the neutrino luminosities would suffer gravitational redshift. However, De Nisco et al. [25] and Bruenn et al. [26] pointed out that GR hydrodynamics produces higher core neutrino luminosities with harder spectra. This gain in the neutrino intensity outweighs the detrimental GR effects in the postbounce evolution of a 13 $M_\odot$ progenitor (Liebendörfer [27]).

Recently, postbounce evolution was reexamined with Boltzmann neutrino transport apart from invoking multidimensional effects. These simulations led to an explosion of a 13 $M_\odot$ progenitor (Liebendörfer [27], Mezzacappa et al. [28]) and to an enhanced shock radius in the failed explosion of a 15 $M_\odot$ progenitor (Rampp [29], Rampp and Janka [30]). It is the purpose of this Letter to report that the increased neutrino luminosities obtained with GR hydrodynamics, together with the improved heating efficiency due to accurate Boltzmann neutrino transport, lead to a powerful supernova explosion in spherical symmetry.

II. GENERAL RELATIVISTIC RADIATION HYDRODYNAMICS

We model the spherically symmetric core collapse, bounce, and postbounce evolution of a 13 $M_\odot$ star, beginning with the precollapse model of Nomoto and Hashimoto [31]. We use the Lattimer-Swesty equation

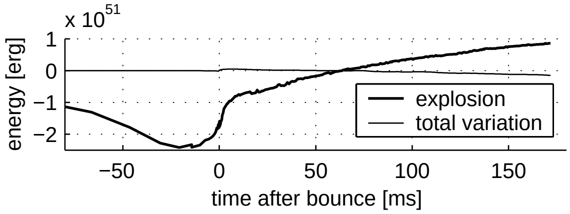

FIG. 1. Plotted versus time is the energy of the matter between the neutrinospheres (energy- and electron-flavor-averaged) and the outer boundary of the computational grid. This energy is well defined prior to and after explosion, and provides a measure of marginality in the case of a failed explosion. Also shown is the drift in the total energy as given by Eq. (1).

of state [7]. Simplified silicon burning is included as described in Ref. [28]. The simulations were carried out with a new general relativistic neutrino radiation hydrodynamics code, AGILE-BOLTZTRAN.

AGILE is an implicit GR hydrodynamics code using an adaptive grid technique to conservatively implement shift vectors in spherical symmetry [32,27]. BOLTZTRAN is an implicit three-flavor multigroup Boltzmann neutrino transport solver [14,33] that was consistently coupled to AGILE, enabled for adaptive gridding, and extended to GR flows [27]. We chose the same discretization in space and neutrino-momentum phase space as in the NR case [28]. The comments on numerical convergence given in Ref. [28] apply as well to the present GR simulation.

We emphasize at this point that the energy evolution in Lagrangian radiation hydrodynamics obeys the very simple conservation equation

$$\frac{\partial}{\partial t}\left[\Gamma\epsilon+\frac{2}{\Gamma+1}\left(\frac{1}{2}U^2-\frac{m}{R}\right)+\Gamma J+UH\right]$$
$$+\frac{\partial}{\partial r}\left[4\pi R^2 e^{\Phi}Up+4\pi R^2 e^{\Phi}n\left(UK+\Gamma H\right)\right]=0. \qquad (1)$$

The variables are defined as in Ref. [4] with the exception that J, H, and K represent the zeroth, first, and second angular moments of the *specific* radiation energy. The integration of Eq. (1) over the total rest mass in the computational domain provides a check on the conservation of total energy, which can easily be monitored as shown in Figure 1.

III. THE ÉLAN IN THE EXPLOSION OF A 13 $M_\odot$ STAR

In the present simulation, the shock forms at an enclosed mass of 0.51 $M_\odot$, i.e., 0.13 $M_\odot$ deeper than in the NR simulation. The shock has to deliver an additional dissociation energy ~ 2 foe (1 foe $= 10^{51}$ erg) while ploughing through this matter. However, the energy and lepton release in the neutrino burst (as the shock crosses the neutrinospheres) completely drains the shock in both the GR and NR simulations, ruling out a “prompt” hydrodynamic explosion in either case. Moreover, the different amounts of undissociated matter inside the shock in the GR and NR simulations influence the energy budget only for a limited time because they either make the transition to bulk nuclear matter or are dissociated due to compressional heating in the compactifying core. Thus, at about 30 ms after bounce, we are left with almost identical states in the GR and NR simulations, with an accretion shock at the edge of the original iron core at a radius ~ 120 km. The only marked difference is the hotter core temperature in the GR case.

The ensuing evolution is driven by neutrino heating. The heating rate essentially depends on the intensity of the neutrino source, the transport from the source to the heating region (subject to redshift), and the absorption efficiency. We distinguish these primary driving forces from secondary contributors, which themselves depend on the postbounce evolution. For example, the accretion-induced neutrino luminosities, the infall velocity in the heating region, and the motion of the neutrinospheres are subject to a self-regulatory feedback in the spirit of Burrows and Goshy [34].

Focusing on the driving forces: (i) The more compact core in the GR simulation has a higher binding energy, which leads to larger core internal energies and temperatures. This in turn leads to higher core luminosities in all neutrino flavors (Bruenn et al. [26]). (ii) The solution of the exact Boltzmann equation for the neutrino transport reproduces accurately the isotropy of the neutrino radiation field. An increased isotropy in the semi-transparent regime keeps the outstreaming neutrinos longer in the heating region and therefore increases the absorption efficiency with respect to the multigroup flux-limited diffusion approximation (Messer et al. [35], Yamada et al. [36]). (iii) The neutrinos in curved spacetime propagate on trajectories with nearly constant $\varepsilon=(\Gamma+U\mu)E$ and $b=R\sqrt{1-\mu^2}/(\Gamma+U\mu)$, where μ and E are the neutrino propagation-angle cosine and energy measured by comoving observers. These GR corrections for redshift and curvature between the neutrinospheres and the heating region do not exceed 3% during the onset of the explosion and increase only later, when the neutrinospheres have receded to smaller radii.

In Figure 2, we plot the electron-flavor neutrino luminosities and rms energies in the heating region at a radius of 100 km as a function of time. We have also included the corresponding quantities from the NR simulation for comparison. We find an increase in the rms energies $\sim 10\%$ and an increase in the luminosities $\sim 30\%$ in the initial heating phase. The luminosity increase is greater for the electron antineutrinos. Although the cooling is also increased in the GR simulation, the substan-

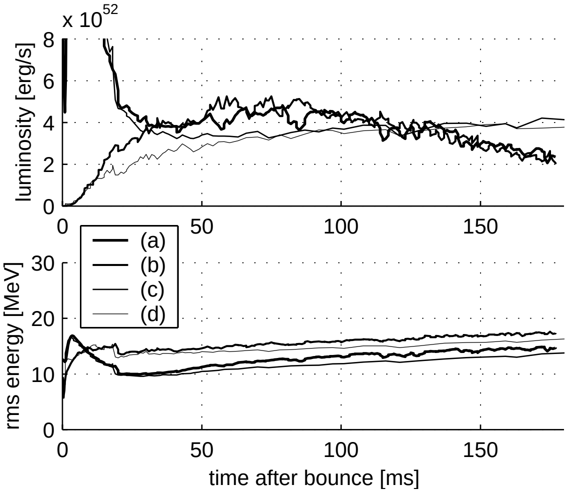

FIG. 2. Neutrino luminosities and rms energies versus time at a radius of 100 km for the GR and NR simulations. The labels are: (a) GR neutrino, (b) GR antineutrino, (c) NR neutrino, and (d) NR antineutrino.

tially larger heating dominates.

Figure 3 shows the mass density, entropy per baryon, electron fraction, and velocity as a function of radius for various time slices in our simulation. In comparison with the NR simulation, we find a much faster initial increase in the entropy and electron fraction, indicating more efficient heating. However, the earlier onset of an explosion prevents the entropies and electron fractions from reaching the high levels observed in the weaker explosion of the NR simulation. The simulation was stopped at 187 ms after bounce when the explosion energy (as defined in Ref. [28]) reached 1 foe. At this time, the explosion energy is rising at the rate of 0.04 foe/10 ms.

IV. CONCLUSION AND OUTLOOK

We have simulated the spherically symmetric, general relativistic core collapse, bounce, and supernova explosion of a 13 $M_\odot$ progenitor. The confluence of (i) the GR core hydrodynamic structure acting as a more intense neutrino source and (ii) the increased heating efficiency obtained from accurate three-flavor Boltzmann neutrino transport leads to an energetic supernova explosion with an explosion energy exceeding 1 foe. In contrast to the two-shock explosion scenario in our NR simulation [28], the radius-versus-time trajectories of equal mass shells in Figure 4 exhibit a one-shock scenario. The revival of the accretion shock by the expansion of the neutrino heated matter in region C is best seen by the reappearance of positive postshock velocities in Figure 3d. The masscut is in the iron core at 1.15 $M_\odot$.

It is tempting to speculate that the increase of more

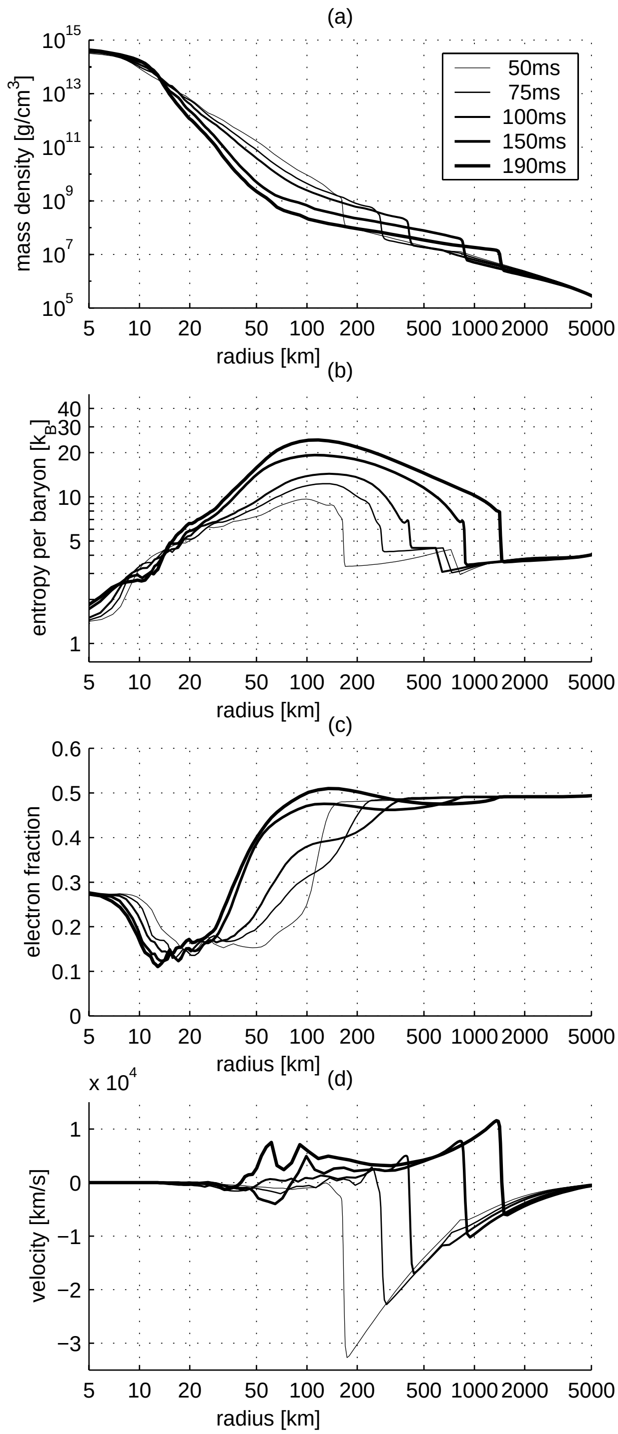

FIG. 3. Baryon density, entropy per baryon, electron fraction, and velocity profiles at select times during the GR simulation.

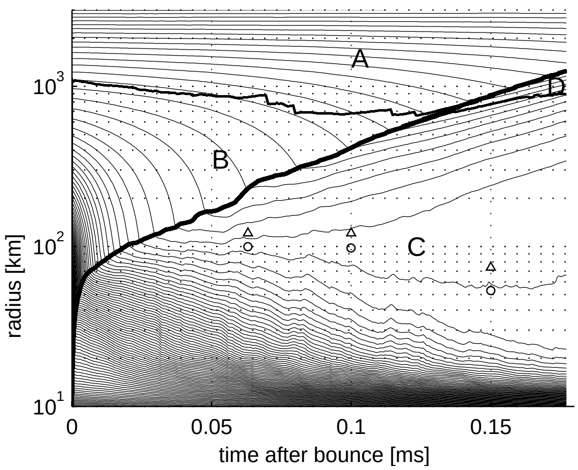

FIG. 4. Radial trajectories of equal mass shells (0.01 $M_{\odot}$) in the iron core and silicon layer. We trace the shock, nuclear burning, and dissociation fronts, which carve out four regions in the (r, t) plane. A: Silicon. B: Iron produced by infall compression and heating. C: Free nucleons and alpha particles. D: Iron and alpha particles produced by shock compression and heating. At three select times, the gain radii (circles) and radii of peak neutrino heating (triangles) are shown.

than 0.6 foe in explosion energy between the NR and the GR simulation would carry over to and be sufficient to successfully explode larger cores. It, however, remains to be investigated if the difference in explosion energy is not mainly due to the qualitatively different explosion scenarios, the intrinsically more energetic one-shock scenario being selected by the beneficial GR effects we have discussed. We are in the process of carrying out simulations with other progenitor models.

ACKNOWLEDGMENTS

M.L. is supported by the National Science Foundation under contract AST-9877130 and, formerly, was supported by the Swiss National Science Foundation under contract 2000-53798.98. A.M. is supported at the Oak Ridge National Laboratory, managed by UT-Battelle, LLC, for the U.S. Department of Energy under contract DE-AC05-00OR22725. F.-K.T. is supported in part by the Swiss National Science Foundation under contract 2000-53798.98 and as a Visiting Distinguished Scientist at the Oak Ridge National Laboratory. O.E.B.M. is supported by funds from the Joint Institute for Heavy Ion Research and a Dept. of Energy PECASE award. W.R.H. is supported by NASA under contract NAG5-8405 and by funds from the Joint Institute for Heavy Ion Research. S.W.B. is supported by the NSF under contract 96-18423 and by NASA under contract NAG5-3903. Our simulations were carried out on the ORNL Physics Division Cray J90 and the National Energy Research Supercomputer Center Cray J90 and SV-1.

---

[1] S. A. Colgate and R. H. White, Astrophysical Journal **143**, 626 (1966).

[2] M. M. May and R. H. White, Computational Physics **7**, 219 (1967).

[3] C. W. Misner and D. H. Sharp, Physical Review **136**, B571 (1964).

[4] R. W. Lindquist, Annals of Physics **37**, 487 (1966).

[5] J. R. Wilson, Astrophysical Journal **163**, 209 (1971).

[6] E. Baron, J. Cooperstein, and S. Kahana, Nuclear Physics A **440**, 744 (1985).

[7] J. Lattimer and F. D. Swesty, Nuclear Physics **A535**, 331 (1991).

[8] P. J. Schinder and S. L. Shapiro, Astrophysical Journal Supplement Series **50**, 23 (1982).

[9] S. W. Bruenn, Astrophysical Journal Supplement Series **58**, 771 (1985).

[10] A. Burrows and J. M. Lattimer, Astrophysical Journal **307**, 178 (1986).

[11] W. D. Arnett, Astrophysical Journal **218**, 815 (1977).

[12] R. L. Bowers and J. R. Wilson, Astrophysical Journal Supplement Series **50**, 115 (1982).

[13] E. S. Myra, S. A. Bludman, Y. Hoffman, I. Lichtenstadt, N. Sack, and K. A. Van Riper, Astrophysical Journal **318** 744 (1987).

[14] A. Mezzacappa and S. W. Bruenn, Astrophysical Journal **405**, 637 (1993).

[15] A. Mezzacappa and S. W. Bruenn, Astrophysical Journal **410**, 740 (1993).

[16] S. W. Bruenn and T. Dineva, Astrophysical Journal Letters **458**, L71 (1996).

[17] J. R. Wilson and R. W. Mayle, Physics Reports **227**, 97 (1993).

[18] M. Herant, W. Benz, and S. A. Colgate, Astrophysical Journal **395**, 642 (1992).

[19] D. S. Miller, J. R. Wilson, and R. W. Mayle, Astrophysical Journal **415**, 278 (1993).

[20] M. Herant, W. Benz, R. W. Hix, C. L. Fryer, and S. A. Colgate, Astrophysical Journal **435**, 339 (1994).

[21] A. Burrows, J. Hayes, and B. A. Fryxell, Astrophysical Journal **450**, 830 (1995).

[22] H.-T. Janka and E. Müller, Astronomy and Astrophysics **306**, 167 (1996).

[23] W. Keil, H.-T. Janka, and E. Müller, Astrophysical Journal Letters **473**, L111 (1996).

[24] A. Mezzacappa, A. C. Calder, S. W. Bruenn, J. M. Blondin, M. W. Guidry, M. R. Strayer, and A. S. Umar, Astrophysical Journal **493**, 848; and **495**, 911 (1998).

[25] K. De Nisco, S. W. Bruenn, and A. Mezzacappa, American Astronomical Society Meeting, 191, #39.10 (1997).

[26] S. W. Bruenn, K. R. DeNisco, and A. Mezzacappa, Astrophysical Journal, submitted (2000).

[27] M. Liebendörfer, Ph.D. thesis, University of Basel, Basel,

Switzerland, 2000.
[28] A. Mezzacappa, M. Liebendörfer, O. E. B. Messer, R. W. Hix, F.-K. Thielemann, and S. W. Bruenn, Physical Review Letters, submitted astro-ph/0005366 (2000).
[29] M. Rampp, Ph.D. thesis, TU München, München, Germany, (2000).
[30] M. Rampp and H.-T. Janka, Astrophysical Journal Letters, submitted astro-ph/0005438 (2000).
[31] K. Nomoto and M. Hashimoto, Physics Reports **163**, 13 (1988).
[32] M. Liebendörfer and F.-K. Thielemann, in *Nineteenth Texas Symposium on Relativistic Astrophysics*, edited by E. Aubourg, T. Montmerle, J. Paul, and P. Peter (Elsevier Science B. V., Amsterdam, 2000).
[33] A. Mezzacappa and O. E. B. Messer, Journal of Computational and Applied Mathematics **109**, 281 (1998).
[34] A. Burrows and J. Goshy, Astrophysical Journal Letters **416**, L75 (1993).
[35] O. E. B. Messer, A. Mezzacappa, S. W. Bruenn, and M. W. Guidry, Astrophysical Journal **507**, 353 (1998).
[36] S. Yamada, H.-T. Janka, and H. Suzuki, Astronomy and Astrophysics **344**, 533 (1999).

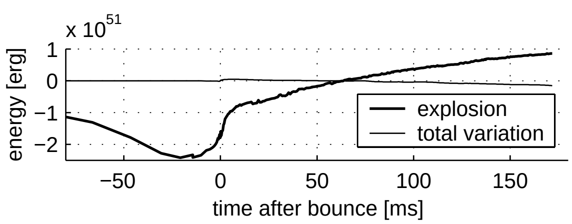

x 10^51
energy [erg]
1
0
−1
−2
−50
0
50
100
150
time after bounce [ms]
explosion
total variation

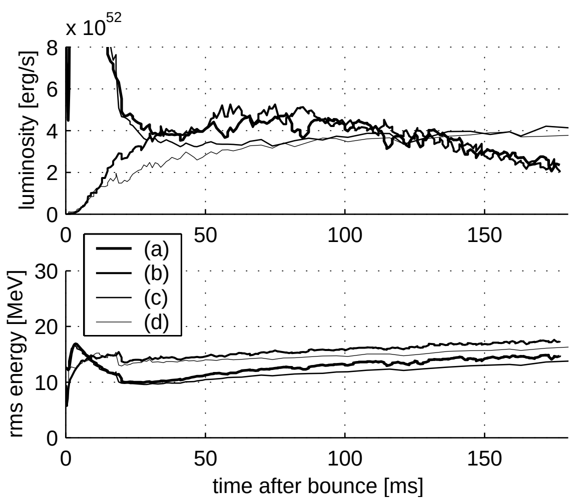
x 10^52
luminosity [erg/s]
8
6
4
2
0
0
50
100
150
(a)
(b)
(c)
(d)
rms energy [MeV]
30
20
10
0
0
50
100
150
time after bounce [ms]

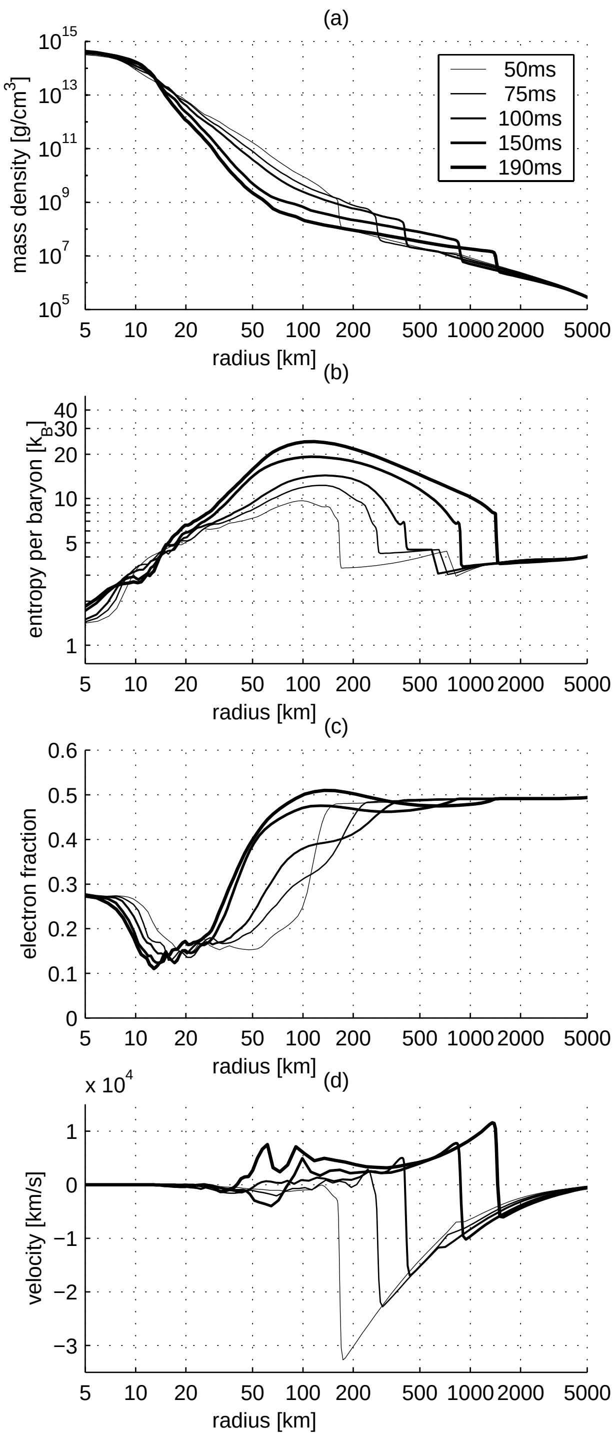
(a)
mass density [g/cm3]
50ms
75ms
100ms
150ms
190ms
radius [km]
(b)
entropy per baryon [kB]
radius [km]
(c)
electron fraction
radius [km]
(d)
x 10^4
velocity [km/s]
radius [km]

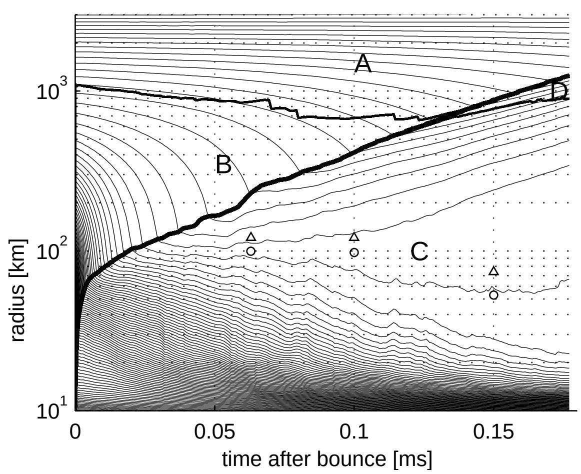

A
B
C
D
radius [km]
time after bounce [ms]
10^1
10^2
10^3
0
0.05
0.1
0.15